

## DIFFRACTION TOMOGRAPHY USING ARBITRARY TRANSMITTER AND RECEIVER SURFACES<sup>1</sup>

A. J. Devaney and G. Beylkin

Schlumberger-Doll Research  
P. O. Box 307  
Ridgefield, CT 06877

The theory of diffraction tomography for two-dimensional objects within the Born approximation is presented for cases where the scattered field is measured over arbitrarily shaped boundaries surrounding the object. Reconstruction algorithms are presented for both plane wave (parallel beam) and cylindrical wave (fan beam) insonification. Special attention is devoted to cases where the measurement and source boundaries are either lines or circles. The theory and algorithms presented are shown to be readily extended to the case of three-dimensional objects.

**Key words:** Diffraction tomography; filtered backpropagation; fan beam tomography

### 1. INTRODUCTION

The theory of diffraction tomography within the Born and Rytov approximations is usually developed for the parallel beam, classical tomographic geometry illustrated in figure 1 [1-5]. For this geometry the object is insonified by a plane wave and the scattered field is measured over a plane surface which is parallel with the incident wavefront. The receiver surface rotates about a central point in the object as different directions of insonification are employed and the goal is to reconstruct the object's properties (eg., acoustic velocity profile) from the set of scattered field measurements so obtained.

In this paper we consider more general experimental geometries such as are illustrated in figures 2 and 3. In figure 2 the object is still insonified by plane waves but the scattered field measurements are performed over arbitrarily shaped surfaces surrounding the object- one surface for each direction of plane wave insonification. In figure 3 the object is surrounded by an arbitrarily shaped surface  $\Sigma_0$  on which are placed point sources. The scattered field measurements are then performed over arbitrarily shaped surfaces surrounding the object- one surface for each location of the point source. In the case of figure 2 the object's properties are to be reconstructed from the totality of scattered field measurements performed in a sequence of experiments employing a full or partial set of insonifying plane waves. In the case of figure 3 the reconstruction is to be performed from the scattered field data generated as the point source covers a whole or part of the surface  $\Sigma_0$ . In either case the measurement surface  $\Sigma$  can remain fixed throughout the sequence of experiments or, alternatively, can vary from experiment to experiment.

A brief review of the foundations of diffraction tomography within the Born approximation is presented in Section 2. For the sake of simplicity only two-dimensional objects will be considered here and throughout the remainder of the paper. The final section describes how the results obtained in the paper can be generalized to the three-dimensional case. The plane wave **scattering amplitude** of an acoustic object is defined and shown to be proportional to the spatial Fourier transform of the "object profile" evaluated on circles in Fourier space which are the two-dimensional analogues of the well known Ewald spheres of X-ray crystallography [6,7]. For the classical tomographic configuration shown in figure 1 the scattering amplitude is also shown to be proportional to the spatial Fourier transform of the scattered field over the measurement line. Finally, an inversion formula is presented that allows the object profile to be reconstructed from the scattering amplitude specified over a range of insonifying wave directions. For the classical tomographic configuration the scattering amplitude can be expressed in terms of the scattered field

<sup>1</sup> A preliminary account of some of the material considered in this paper was presented at the 13th International Acoustical Imaging Symposium, October 26-28, 1983.

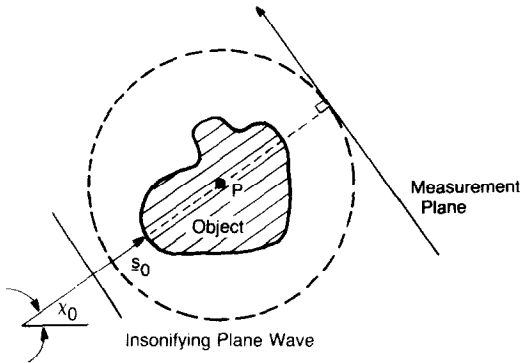


Fig. 1 Classical tomographic configuration. Measurement plane rotates about a central point "P" remaining always parallel with the insonifying plane wavefront.

over the measurement line and the inversion formula reduces to the filtered backpropagation algorithm of parallel beam ultrasound tomography [4,5].

The case of plane wave insonification with an arbitrary measurement boundary is considered in Section 3. A mathematical identity relating the value of the field and its normal derivative on the measurement boundary  $\Sigma$  to the scattering amplitude of the object is derived. For cases where the measurement boundary is either a straight line or circle, the identity simplifies and does not involve the normal derivative of the field on the boundary. A similar simplification is shown to hold approximately for boundaries whose curvature is small relative to a wavelength. By employing the appropriate identity in conjunction with the inversion formula presented in Section 2, a two-step algorithm is obtained for reconstructing the object profile from the scattered field data.

Section 4 addresses the configuration illustrated in figure 3. An identity relating the plane wave scattering amplitude to the cylindrical wave scattering amplitude of the object is derived for the three cases where the source surface  $\Sigma_0$  is one or more straight lines, a circle, or a general shape whose curvature is small relative to a wavelength- the identity for this last case being approximate. These identities allow the inversion formula presented in Section 2 to be employed since they convert scattered field data generated by cylindrical insonifying waves (fan beams) to scattered field data generated by insonifying plane waves. By employing these identities in conjunction with the inversion formula a "fan beam" reconstruction algorithm is obtained that allows the object profile to be directly reconstructed from cylindrical wave scattered field data measured over arbitrary boundaries surrounding the object. The final section of the paper briefly addresses the case of three-dimensional objects and discusses applications for the algorithms presented in the paper.

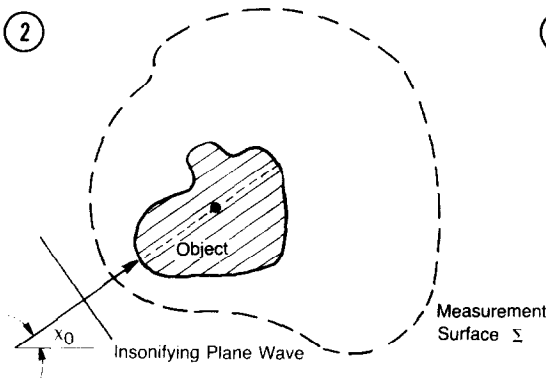


Fig. 2 Parallel beam insonification with arbitrary shaped measurement surface  $\Sigma$ .

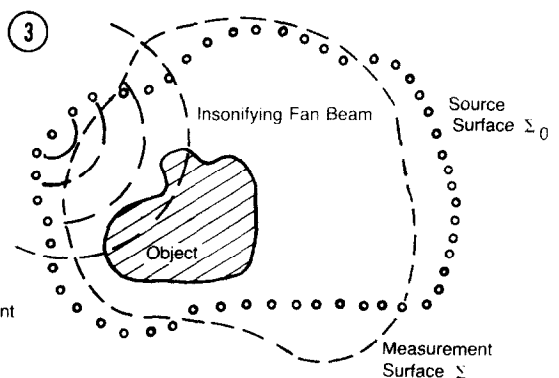


Fig. 3 Fan beam insonification with arbitrary shaped measurement surface  $\Sigma$  and arbitrary source surface  $\Sigma_0$ .

2. DIFFRACTION TOMOGRAPHY WITHIN THE BORN APPROXIMATION

We consider the situation illustrated in figure 2 of an acoustic object surrounded by an arbitrary measurement surface  $\Sigma$ . We shall limit our attention to those applications where the wave propagation is governed by the inhomogeneous Helmholtz equation

$$(\nabla^2 + k^2)\psi(\underline{r}) = k^2 O(\underline{r})\psi(\underline{r}) . \tag{1}$$

Here,  $k = \omega/C_0$  is the wavenumber of the field in the medium surrounding the object at frequency  $\omega$  and  $O(\underline{r})$  is the "object profile." For acoustic scattering, Eq. (1) applies if the density of the object is constant and equal to that of the embedding medium and if the shear modulus of the object and embedding medium are negligible [2]. The theory and results developed below can, however, be generalized to the non-constant density case following the treatment presented in [8].

As discussed earlier, we shall restrict our attention here and throughout the remainder of the paper to two-dimensional objects; i.e., objects whose properties are constant in one direction (say the z axis) but vary in perpendicular directions (say over the x-y plane). We will also assume that the object is insonified by a wave that is also constant along the z direction. In this and the following section, the insonifying wave is a plane wave whose unit propagation vector  $\underline{s}_0$  lies in the x-y plane. Cylindrical waves having axes aligned parallel to the z axis are considered in Section 4. For both of these cases the field  $\psi(\underline{r})$  will depend only on the x-y coordinates so that the wave equation (1) is a two-dimensional equation.

The object profile  $O(\underline{r})$  is the quantity which is to be determined in diffraction tomography. This quantity is related to the velocity profile  $C(\underline{r})$  of the object through the equation [4]

$$O(\underline{r}) = 1 - \frac{C_0^2}{C^2(\underline{r})} , \tag{2}$$

where  $C_0$  is the velocity of the embedding medium. In general, the velocity  $C(\underline{r})$  will be complex so that a reconstruction of  $O(\underline{r})$  yields both the phase velocity and attenuation profiles of the object.

The goal of diffraction tomography is to reconstruct  $O(\underline{r})$  from scattered field measurements. The most compact and convenient form of such data is given by the so-called plane wave scattering amplitude of the object. For the case of two-dimensional objects, the plane wave scattering amplitude is defined via the equation

$$f(\underline{s}, \underline{s}_0) \equiv k^2 \int d^2r O(\underline{r})\psi(\underline{r}; \underline{s}_0) e^{-i\kappa s \underline{r}} , \tag{3}$$

where  $\underline{s}_0$  and  $\underline{s}$  are two-dimensional unit vectors that can range over the entire unit circle. In the above definition  $\psi(\underline{r}; \underline{s}_0)$  is the total field (incident plus scattered) generated by an insonifying plane wave whose unit propagation vector is  $\underline{s}_0$ . Throughout this and the following section we shall refer to  $f(\underline{s}, \underline{s}_0)$  as simply the "scattering amplitude."

For certain measurement geometries, the scattering amplitude  $f(\underline{s}, \underline{s}_0)$  is readily determined from scattered field measurements. For example, for the classical tomographic configuration illustrated in figure 1, the value of the forward scattered field over the measurement line determines  $f(\underline{s}, \underline{s}_0)$  for those values of  $\underline{s}$  lying on the half unit circle  $\underline{s} \cdot \underline{s}_0 \geq 0$ . More specifically, one finds that for  $\underline{s} \cdot \underline{s}_0 \geq 0$  [9]

$$f(\underline{s}, \underline{s}_0) = 2i \gamma e^{-i\gamma l_0} \int_{-\infty}^{\infty} d\xi' \psi^{(s)}(\xi'; \underline{s}_0) e^{-i\kappa \xi'} , \tag{4}$$

where  $\xi'$  denotes position along the measurement line and  $\psi^{(s)}(\xi'; \underline{s}_0)$  is the scattered field at the point  $\xi'$  and  $\kappa$  and  $\gamma$  are, respectively, the projections of  $k \underline{s}$  onto the measurement line and onto

the direction of  $\underline{s}_0$ ; i.e.,

$$\kappa = k\underline{s} \cdot \hat{\underline{\xi}} \quad (5a)$$

$$\gamma = k\underline{s} \cdot \underline{s}_0 = \sqrt{k^2 - \kappa^2}, \quad (5b)$$

where  $\hat{\underline{\xi}}$  denotes the unit vector in the positive  $\xi$  direction. (Recall that for the classical tomographic configuration the measurement line is perpendicular to  $\underline{s}_0$  so that  $\hat{\underline{\xi}} \cdot \underline{s}_0 = 0$ .) Porter [10] has generalized (4) to the case of arbitrarily shaped measurement boundaries. As shown by Porter, the generalization to such cases requires, in general, that **both** the scattered field and its normal derivative **be measured** over the surface. We shall present, in the following section, a generalization of Eq. (4) to arbitrarily shaped measurement boundaries that differs somewhat from the extension proposed by Porter [10].

The scattering amplitude plays a fundamental role in inverse scattering and diffraction tomography. Within the Born approximation,  $f(\underline{s}, \underline{s}_0)$  reduces to the two-fold spatial Fourier transform of  $O(\underline{r})$  evaluated over certain circular boundaries in Fourier space (Ewald spheres in the three-dimensional case). This result follows immediately upon substituting the insonifying field  $\exp(i k \underline{s}_0 \cdot \underline{r})$  for  $\psi(\underline{r}; \underline{s}_0)$  in Eq. (3) (i.e., making the Born approximation). We obtain [4]

$$f(\underline{s}, \underline{s}_0) \approx k^2 \int d^2 \underline{r} O(\underline{r}) e^{-i k (\underline{s} - \underline{s}_0) \cdot \underline{r}} = k^2 \tilde{O}[k(\underline{s} - \underline{s}_0)], \quad (6)$$

where

$$\tilde{O}(\underline{K}) \equiv \int d^2 \underline{r} O(\underline{r}) e^{-i \underline{K} \cdot \underline{r}} \quad (7)$$

denotes the two-fold spatial Fourier transform of the object profile.

Eq. (6) states that the scattering amplitude  $f(\underline{s}, \underline{s}_0)$  determines the two-fold Fourier transform of the object profile over the locus of  $\underline{K}$  values defined by the equation

$$\underline{K} = k(\underline{s} - \underline{s}_0). \quad (8)$$

For fixed  $k$  and  $\underline{s}_0$ , Eq. (8) defines a locus of  $\underline{K}$  values lying on a circle centered at  $\underline{K} = -k\underline{s}_0$  and having a radius equal to  $k$ . As discussed in references 4 and 5, the above result is, essentially, the generalization of the projection-slice theorem of x-ray tomography to diffraction tomography and forms the basis for all reconstruction algorithms presently employed in diffraction tomography. For example, for the conventional tomographic configuration  $f(\underline{s}, \underline{s}_0)$  is determined for unit vectors  $\underline{s}$  satisfying  $\underline{s} \cdot \underline{s}_0 \geq 0$  from forward scatter measurement via Eq. (4). By varying  $\underline{s}_0$  (i.e., changing the direction of insonification) a set of semicircular arcs in Fourier space are obtained over which the data specifies the transform  $\tilde{O}(\underline{K})$ .  $O(\underline{r})$  can then be estimated from this information using, for example, interpolation followed by Fourier inversion [1, 11-13].

An inversion formula has been derived recently which allows  $O(\underline{r})$  to be reconstructed directly from the scattering amplitude without the need of interpolation or Fourier inversion. In the case of two-dimensional objects the formula is given by [4, 5, 14]

$$O_{LP}(\underline{r}) = \frac{1}{2(2\pi)^2} \int_{-\pi}^{\pi} d\chi_0 \int_{-\pi}^{\pi} d\chi \sqrt{1 - (\underline{s} \cdot \underline{s}_0)^2} f(\underline{s}, \underline{s}_0) e^{i k (\underline{s} - \underline{s}_0) \cdot \underline{r}}, \quad (9)$$

where  $\chi_0$  and  $\chi$  are, respectively, the angles formed by  $\underline{s}_0$  and  $\underline{s}$  with a fixed reference direction. The subscript "LP" on  $O(\underline{r})$  means that a "low pass filtered" approximation to the object profile is obtained; i.e.,

$$O_{LP}(\underline{r}) = \frac{1}{(2\pi)^2} \int_{K < 2k} d^2 \underline{K} \tilde{O}(\underline{K}) e^{i \underline{K} \cdot \underline{r}}. \quad (10)$$

The inversion formula (9) forms the basis for the filtered backpropagation algorithm for parallel beam insonification. This algorithm corresponds, essentially, to a decomposition of the formula (9) into two steps: (i) forming a partial reconstruction at fixed view angle (angle of insonification  $\chi_0$ ); (ii) summing over view angles. We define the partial reconstruction as

$$\hat{O}(\underline{r}; \chi_0) \equiv \frac{1}{4\pi} \int_{-\pi}^{\pi} d\chi \sqrt{1 - (\underline{s} \cdot \underline{s}_0)^2} f(\underline{s}, \underline{s}_0) e^{ik(\underline{s} - \underline{s}_0) \cdot \underline{r}}. \quad (11a)$$

It then follows from Eq. (9) that  $O_{LP}(\underline{r})$  is given by

$$O_{LP}(\underline{r}) = \frac{1}{2\pi} \int_{-\pi}^{\pi} d\chi_0 \hat{O}(\underline{r}; \chi_0). \quad (11b)$$

The construction of  $\hat{O}(\underline{r}; \chi_0)$  according to Eq. (11a) can be interpreted as a filtered backpropagation process while Eq. (11b) represents a sum over view angles [4, 5].

### 3. PARALLEL BEAM INSONIFICATION

Our primary goal in this section is to provide a formula for determining the scattering amplitude from field measurements performed over the arbitrary measurement boundary  $\Sigma$ . The function  $f(\underline{s}, \underline{s}_0)$  so obtained can then be employed in Eq. (9) (or, equivalently in Eqs. (11)) to obtain a reconstruction of the object profile.

Porter [10] has addressed this problem and proposed a scheme which is a two-step procedure requiring first that a holographic image be formed from the measured field followed by a spatial Fourier transformation of this image field. We shall employ a more direct method that avoids entirely these two steps. We make use of the following integral identity which is derived in Appendix A.

$$\begin{aligned} & k^2 \int d^2r' O(\underline{r}') \psi(\underline{r}') e^{-ik\underline{s} \cdot \underline{r}'} \\ &= \int_{\Sigma} dl' [ik \hat{\underline{n}}' \cdot \underline{s} \psi^{(s)}(\underline{r}') + \frac{\partial}{\partial n'} \psi^{(s)}(\underline{r}')] e^{-ik\underline{s} \cdot \underline{r}'}. \end{aligned} \quad (12)$$

In this equation  $\underline{s}$  is a unit vector that can span the unit circle,  $dl'$  is the differential length element on  $\Sigma$ ,  $\hat{\underline{n}}'$  the unit outward normal vector to  $\Sigma$  at the point  $\underline{r}'$  and  $\frac{\partial}{\partial n'}$  denotes the derivative along the  $\hat{\underline{n}}'$  direction. The field  $\psi(\underline{r}')$  is the total field (incident plus scattered) generated by any incident wave to the object  $O(\underline{r})$  and  $\psi^{(s)}$  is the scattered wave component of  $\psi$ ; i.e., the total field minus the incident field.

Since  $\psi(\underline{r}')$  is the total field generated by any incident wave to the object we are free to choose the incident wave to be the plane wave  $\exp(ik\underline{s}_0 \cdot \underline{r}')$ . For this choice  $\psi(\underline{r}') = \psi(\underline{r}', \underline{s}_0)$  and the left-hand side of Eq. (12) reduces to the scattering amplitude. We then have the result

$$f(\underline{s}, \underline{s}_0) = \int_{\Sigma} dl' [ik \hat{\underline{n}}' \cdot \underline{s} \psi^{(s)}(\underline{r}', \underline{s}_0) + \frac{\partial}{\partial n'} \psi^{(s)}(\underline{r}', \underline{s}_0)] e^{-ik\underline{s} \cdot \underline{r}'}. \quad (13)$$

Eq. (13) allows the scattering amplitude to be evaluated directly in terms of the scattered field and its normal derivative over an arbitrary boundary  $\Sigma$  surrounding the object. This equation when coupled to Eq. (9) then provides a two step inversion formula for reconstructing  $O(\underline{r})$  from  $\psi^{(s)}$  and its normal derivative evaluated over  $\Sigma$ . Unfortunately, in most applications, it is not possible to measure **both**  $\psi^{(s)}$  and  $\frac{\partial}{\partial n'} \psi^{(s)}$  on  $\Sigma$ . Moreover, in theory it is not necessary since it can be shown that either one alone uniquely determines the other [15].

In practice it is possible to obtain an exact relationship between the scattering amplitude  $f(\underline{s}, \underline{s}_0)$  and either  $\psi^{(s)}$  or  $\frac{\partial}{\partial n'} \psi^{(s)}$  only for boundaries which coincide with one of the coordinate axes of a curvilinear coordinate system in which the Helmholtz equation separates [15]. Important examples of such boundaries, called "separable boundaries", are circles and infinite straight lines. For example, for a straight line boundary perpendicular to  $\underline{s}_0$ , Eq. (13) reduces to Eq. (4). This follows from the fact that over any line, independent of its orientation, the integral involving  $\psi^{(s)}$  in Eq. (13) exactly cancels the integral involving  $\frac{\partial}{\partial n'} \psi^{(s)}$  if  $\hat{n}' \cdot \underline{s} < 0$ , and the two are equal if  $\hat{n}' \cdot \underline{s} \geq 0$  [16]. Thus, we have the general result that for all  $\underline{s}$  such that  $\hat{n}' \cdot \underline{s} \geq 0$

$$f(\underline{s}, \underline{s}_0) = 2ik \hat{n}' \cdot \underline{s} \int_{-\infty}^{\infty} dl' \psi^{(s)}(l'; \underline{s}_0) e^{-iks l'} \quad (14)$$

where we have denoted by  $\psi^{(s)}(l'; \underline{s}_0)$  the scattered field  $\psi^{(s)}(\underline{r}'; \underline{s}_0)$  evaluated on the measurement line. Eq. (4) is then a special case of (14) for the classical tomographic configuration where  $\hat{n}' = \underline{s}_0$ , the direction of propagation of the insonifying plane wave.

For the case of a circular boundary one finds that Eq. (13) reduces to [16]

$$f(\underline{s}, \underline{s}_0) = 4i \int_0^{2\pi} d\sigma \psi^{(s)}(\sigma; \underline{s}_0) F_R(\chi - \sigma) \quad (15)$$

where  $R$  is the radius of the measurement circle  $\Sigma$  assumed to be centered at the origin and  $\sigma$  and  $\chi$  are, respectively, the angles made by  $\underline{r}'$  and  $\underline{s}$  with an arbitrary reference direction.  $\psi^{(s)}(\sigma; \underline{s}_0)$  denotes the scattered field at the angle  $\sigma$  and the function  $F_R(x)$  is given by

$$F_R(x) = \frac{1}{(2\pi)^2} \sum_{n=-\infty}^{\infty} \frac{i^n}{H_n(kR)} e^{inx} \quad (16)$$

where  $H_n$  is the  $n$ 'th order Hankel function of the first kind. It should be noted that the center and radius of  $\Sigma$  can be changed as a function of the insonifying wave vector  $\underline{s}_0$ .

An approximate expression for  $f(\underline{s}, \underline{s}_0)$  for arbitrarily shaped boundaries which involves only the scattered field can be employed if the boundary curvature is such that it can be approximated by a straight line in the vicinity of each point. This requires that the local radius of curvature be much larger than a wavelength. If this condition is met then the arguments leading to Eq. (14) for the case when  $\Sigma$  is a straight line can be applied and Eq. (13) then reduces, approximately, to

$$f(\underline{s}, \underline{s}_0) \approx 2ik \int_{\Sigma} dl' \hat{n}' \cdot \underline{s} \psi^{(s)}(\underline{r}'; \underline{s}_0) e^{-iks l'} \quad (17)$$

where  $\hat{n}' \cdot \underline{s}$  must now remain under the integral sign since  $\hat{n}'$  is not constant for a curved boundary.

#### 4. CYLINDRICAL BEAM INSONIFICATION

In this section we consider the case where the object is insonified by a cylindrical wave generated by a line source located on a closed boundary  $\Sigma_0$  surrounding the object. For parallel beam insonification the object profile is reconstructed from scattered field measurements performed over an arbitrary boundary  $\Sigma$  surrounding the object. A reconstruction of the object profile is obtained from the set of scattered field measurements that result from using different directions of insonification of the incident wave (different unit wave vectors  $\underline{s}_0$ ). For the cylindrical beam case we will also assume that the scattered field is measured over an arbitrary boundary which completely surrounds the object. The object profile reconstruction is then obtained from the set of scattered field measurements that result when the location of the line source varies over  $\Sigma_0$ .

We shall present two alternative schemes for generating a reconstruction of the object profile from cylindrical beam scattering data. The first is a two-step method in which the scattering amplitude is first computed from cylindrical beam scattering data. The object profile is then reconstructed in a second step using the plane wave filtered backpropagation algorithm [4]. The second method combines the two steps into a single mathematical operation. What results is then a filtered backpropagation algorithm where the "sum over view angles" operation is replaced by a "sum over source points" operation. This second method is the diffraction tomographic equivalent of the fan beam filtered backprojection algorithm of x-ray tomography [17].

We begin by defining, in analogy with Eq. (3), the cylindrical wave scattering amplitude  $\gamma(\underline{s}; \underline{R}_o)$  of the object:

$$\gamma(\underline{s}; \underline{R}_o) \equiv k^2 \int d^2\tau O(\underline{r}) \psi(\underline{r}; \underline{R}_o) e^{-ik\underline{s}\cdot\underline{r}}. \quad (18)$$

In Eq. (18)  $\psi(\underline{r}; \underline{R}_o)$  is the total field (incident plus scattered) generated by an insonifying cylindrical wave centered at the point  $\underline{R}_o$  located on  $\Sigma_o$ . The cylindrical wave scattering amplitude plays the same role with respect to insonifying cylindrical waves as does the plane wave scattering amplitude  $f(\underline{s}, \underline{s}_o)$  for insonifying plane waves.

The cylindrical wave scattering amplitude can be computed from the value of the scattered field  $\psi^{(s)}(\underline{r}'; \underline{R}_o)$  and its normal derivative  $\frac{\partial}{\partial n'} \psi^{(s)}(\underline{r}'; \underline{R}_o)$  evaluated over the boundary  $\Sigma$ . In particular, by making use of Eq. (12) we conclude that

$$\gamma(\underline{s}; \underline{R}_o) = \int_{\Sigma} dl' \left[ ik \hat{n}' \cdot \underline{s} \psi^{(s)}(\underline{r}'; \underline{R}_o) + \frac{\partial}{\partial n'} \psi^{(s)}(\underline{r}'; \underline{R}_o) \right] e^{-ik\underline{s}\cdot\underline{r}'}, \quad (19)$$

which is the cylindrical wave counterpart to Eq. (13). Because Eq. (19) is mathematically identical to Eq. (13), the arguments leading to Eqs. (14), (15) and (17) remain valid for Eq. (19). In particular, we have for straight line measurement boundaries the result

$$\gamma(\underline{s}; \underline{R}_o) = 2ik \hat{n}' \cdot \underline{s} \int_{-\infty}^{\infty} dl' \psi^{(s)}(l'; \underline{R}_o) e^{-ik\underline{s}\cdot\underline{r}'} \quad (20a)$$

and for circular boundaries

$$\gamma(\underline{s}; \underline{R}_o) = 4i \int_0^{2\pi} d\sigma \psi^{(s)}(\sigma; \underline{R}_o) F_R(\chi - \sigma), \quad (20b)$$

and, finally, for boundaries with weak curvature:

$$\gamma(\underline{s}; \underline{R}_o) \approx 2ik \int_{\Sigma} dl' \hat{n}' \cdot \underline{s} \psi^{(s)}(\underline{r}'; \underline{R}_o) e^{-ik\underline{s}\cdot\underline{r}'}. \quad (20c)$$

The cylindrical wave scattering amplitude  $\gamma(\underline{s}, \underline{R}_o)$  is seen to be linearly related to the scattered wave  $\psi^{(s)}(\underline{r}'; \underline{R}_o)$  generated by an insonifying cylindrical wave. Moreover, the scattered field  $\psi^{(s)}(\underline{r}'; \underline{s}_o)$  produced by an insonifying plane wave can be shown to be linearly related to the scattered field  $\psi^{(s)}(\underline{r}'; \underline{R}_o)$  produced by line sources located on  $\Sigma_o$ . As a consequence of this, the scattering amplitude  $f(\underline{s}, \underline{s}_o)$  is linearly related to  $\gamma(\underline{s}; \underline{R}_o)$ . In particular, it is shown in Appendix B that the plane wave and cylindrical wave scattering amplitudes are related by

$$f(\underline{s}, \underline{s}_o) = \int_{\Sigma_o} dl'_o \left[ ik \hat{n}'_o \cdot \underline{s}_o \gamma(\underline{s}; \underline{R}_o) - \frac{\partial}{\partial n'_o} \gamma(\underline{s}; \underline{R}_o) \right] e^{ik\underline{s}_o \cdot \underline{R}_o}, \quad (21)$$

where  $dl_o$  is the differential length on  $\Sigma_o$ ,  $\hat{n}_o$  the unit outward normal to  $\Sigma_o$  and  $\frac{\partial}{\partial n_o}$  denotes the derivative along the  $\hat{n}_o$  direction.

Eq. (21) is in the form of a linear mapping between the cylindrical wave scattering amplitude and its derivative with respect to  $n_o$  and the plane wave scattering amplitude  $f(\underline{s}, \underline{s}_o)$ . Since the derivative  $\frac{\partial}{\partial n_o} \gamma(\underline{s}; \underline{R}_o)$  cannot be computed from measurements of  $\psi^{(s)}(\underline{r}; \underline{R}_o)$  for fixed  $\underline{R}_o$ , it is important to remove this quantity from Eq. (21). This can be done exactly for cases where  $\Sigma_o$  is a separable boundary. For example, when  $\Sigma_o$  is a straight line one finds that

$$f(\underline{s}, \underline{s}_o) = -\frac{k}{2} \hat{n}_o \cdot \underline{s}_o \int_{-\infty}^{\infty} dl_o \gamma(\underline{s}; l_o) e^{ik s_o \cdot \underline{R}_o}, \quad (22)$$

with Eq. (22) holding for all  $\underline{s}_o$  such that  $\hat{n}_o \cdot \underline{s}_o \leq 0$  and where  $l_o$  now denotes the location of  $\underline{R}_o$  on the straight line boundary. The relationship between Eqs. (22) and (21) is seen to be entirely analogous to that existing between Eqs. (14) and (13) of Section 2. Indeed, Eq. (22) is derived from (21) using arguments identical to those employed in deriving Eq. (14) from (13).

For the case where  $\Sigma_o$  is a circular boundary centered at the origin one finds that Eq. (21) becomes [16]

$$f(\underline{s}, \underline{s}_o) = \int d\beta \gamma(\underline{s}; \beta) F_{R_o}(\beta - \chi_o), \quad (23)$$

where  $F_{R_o}(x)$  is defined in Eq. (16), with  $R$  replaced by  $R_o$ , and where  $\beta$  and  $\chi_o$  are, respectively, the angles formed by  $\underline{R}_o$  and  $\underline{s}_o$  with an arbitrary reference direction. Finally, for cases where the curvature of the boundary  $\Sigma_o$  is sufficiently small that it can be approximated by a straight line in the vicinity of each point; we have

$$f(\underline{s}, \underline{s}_o) \approx -\frac{k}{2} \int_{\Sigma_o} dl_o \hat{n}_o \cdot \underline{s}_o \gamma(\underline{s}; \underline{R}_o) e^{ik s_o \cdot \underline{R}_o}. \quad (24)$$

Eqs. (19)-(24) allow the plane wave scattering amplitude to be synthesized from cylindrical wave scattering data. The cylindrical wave scattering amplitude is first computed using (19) or (20) and the result is employed in Eqs. (22)-(24) to compute  $f(\underline{s}, \underline{s}_o)$ . By combining these equations, the two steps can be combined into a single integral transform relating the cylindrical wave scattering data directly to the plane wave scattering amplitude. Table I lists these transforms for cases where  $\Sigma$  and  $\Sigma_o$  are straight lines or circles and for cases where the curvature of both boundaries is small.

The transformations listed in table I allow the plane wave scattering amplitude to be synthesized from cylindrical wave scattered field data. Once  $f(\underline{s}, \underline{s}_o)$  is computed the plane wave filtered backpropagation algorithm as embodied in Eqs. (9) or (11) can be employed to obtain a reconstruction of the object profile. An alternative, one step reconstruction algorithm, is readily derived by substituting the transformations listed in table I into Eq. (9) and reorganizing the result. We present in table II the resulting reconstruction algorithms corresponding to the three cases - lines, circles and weakly curving boundaries - covered in table I.

The reconstruction algorithms presented in table II are "fan beam" algorithms in the sense that they operate directly on the measured cylindrical wave scattered field data. Like the plane wave filtered backpropagation algorithm presented in Section 2, they can be decomposed into two sequential operations:

1. Generating a partial reconstruction using data collected in a single scattering experiment.
2. Summing the partial reconstructions obtained in step 1 from different experiments to obtain the final reconstruction.

Eqs. (19)-(24) allow the plane wave scattering amplitude to be synthesized from cylindrical wave scattering data. The cylindrical wave scattering amplitude is first computed using (19) or (20) and



**Table I. Scattering amplitude in different cases of source-receiver geometry**

Geometry	Scattering Amplitude $f(\underline{s}, \underline{s}_0)$
$\Sigma_0, \Sigma$ lines	$= -ik^2(\underline{\hat{n}}_0, \underline{s}_0)(\underline{\hat{n}}', \underline{s}) \int_{-\infty}^{\infty} dl_0 \int_{-\infty}^{\infty} dl' \psi^{(s)}(l'; l_0) e^{-ik(\underline{s}\underline{r}' - \underline{s}_0, \underline{R}_0)}$
$\Sigma_0, \Sigma$ circles	$= 4i \int_{-\pi}^{\pi} d\beta \int_{-\pi}^{\pi} d\sigma \psi^{(s)}(\sigma; \beta) F_R(\chi - \sigma) F_{R_0}(\beta - \chi_0)$
$\Sigma_0, \Sigma$ arbitrary but with weak curvature	$= -ik^2 \int_{-\infty}^{\infty} dl_0(\underline{\hat{n}}_0, \underline{s}_0) \int_{-\infty}^{\infty} dl'(\underline{\hat{n}}', \underline{s}) \psi^{(s)}(\underline{r}', \underline{R}_0) e^{-ik(\underline{s}\underline{r}' - \underline{s}_0, \underline{R}_0)}$

the result is employed in Eqs. (22)-(24) to compute  $f(\underline{s}, \underline{s}_0)$ . By combining these equations, the two steps can be combined into a single integral transform relating the cylindrical wave scattering data directly to the plane wave scattering amplitude. Table I lists these transforms for cases where  $\Sigma$  and  $\Sigma_0$  are straight lines or circles and for cases where the curvature of both boundaries is small.

The transformations listed in table I allow the plane wave scattering amplitude to be synthesized from cylindrical wave scattered field data. Once  $f(\underline{s}, \underline{s}_0)$  is computed the plane wave filtered backpropagation algorithm as embodied in Eqs. (9) or (11) can be employed to obtain a reconstruction of the object profile. An alternative, one step reconstruction algorithm, is readily derived by substituting the transformations listed in table I into Eq. (9) and reorganizing the result. We present in table II the resulting reconstruction algorithms corresponding to the three cases - lines, circles and weakly curving boundaries - covered in table I.

**Table II. Reconstruction formulae in different cases of source-receiver geometry**

Geometry	Reconstruction
$\Sigma_0, \Sigma$ lines	$O_{LP}(\underline{r}) = \int_{-\infty}^{\infty} dl_0 \int_{-\infty}^{\infty} dl' \psi^{(s)}(l'; l_0) G_p(\underline{r}; l', l_0), \text{ where}$ $G_p(\underline{r}; l', l_0) \equiv -\frac{ik^4}{2(2\pi)^2} \int_{-\pi}^{\pi} d\chi_0 \int_{-\pi}^{\pi} d\chi(\underline{\hat{n}}_0, \underline{s}_0)(\underline{\hat{n}}', \underline{s}) \sqrt{1 - (\underline{s}, \underline{s}_0)^2} e^{ik\underline{s}(\underline{r} - \underline{r}')} e^{-ik\underline{s}_0 \cdot (\underline{r} - \underline{R}_0)}$
$\Sigma_0, \Sigma$ circles	$O_{LP}(\underline{r}) = \int_{-\pi}^{\pi} d\beta \int_{-\pi}^{\pi} d\sigma \psi^{(s)}(\sigma; \beta) G_c(\underline{r}; \sigma, \beta), \text{ where}$ $G_c(\underline{r}; \sigma, \beta) \equiv \frac{2ik^2}{(2\pi)^2} \int_{-\pi}^{\pi} d\chi_0 \int_{-\pi}^{\pi} d\chi \sqrt{1 - (\underline{s}, \underline{s}_0)^2} F_R(\chi - \sigma) F_{R_0}(\beta - \chi_0) e^{ik(\underline{s} - \underline{s}_0) \cdot \underline{r}}$
$\Sigma_0, \Sigma$ arbitrary but with weak curvature	$O_{LP}(\underline{r}) \approx \int_{-\infty}^{\infty} dl_0 \int_{-\infty}^{\infty} dl' \psi^{(s)}(\underline{r}', \underline{R}_0) G_p(\underline{r}; \underline{r}', \underline{R}_0), \text{ where}$ $G^p(\underline{r}; \underline{r}', \underline{R}_0) = G_p(\underline{r}; l', l_0)$

The reconstruction algorithms presented in table II are "fan beam" algorithms in the sense that they operate directly on the measured cylindrical wave scattered field data. Like the plane wave filtered backpropagation algorithm presented in Section 2, they can be decomposed into two sequential operations:

1. Generating a partial reconstruction using data collected in a single scattering experiment.
2. Summing the partial reconstructions obtained in step 1 from different experiments to obtain the final reconstruction.

In table II the inner integral represents step 1 while the sum over partial reconstructions is performed by the outer integral. In the plane wave case, the sum over experiments consisted of summing over different insonifying angles  $\chi_0$ . Clearly, for fan beam insonification (cylindrical wave insonification) the sum over experiments corresponds to an integral over source points  $\underline{R}_0$ .

We conclude by remarking that the fan beam reconstruction algorithm for circular boundaries given in table II is the generalization, to diffraction tomography, of the x-ray fan beam algorithm presented, for example, in [17]. The parallel beam filtered backpropagation algorithm of diffraction tomography is known to reduce, in the limit where the wavelength goes to zero, to the filtered backprojection algorithm of x-ray tomography [4]. It should then be expected that the circular boundary fan beam algorithm in table II should, likewise, reduce in this limit to the corresponding X-ray algorithm. We have not yet been able to establish this reduction and consider this an interesting and important future research goal for fan beam diffraction tomography.

## 5. CONCLUDING REMARKS

We have, in this paper, shown how the theory and algorithms of parallel beam diffraction tomography within the Born approximation can be extended to cases where the scattered field is measured over arbitrarily shaped boundaries surrounding the object. In addition, we presented two reconstruction procedures for fan beam diffraction tomography. The first of these is a two-step inversion algorithm where plane wave scattering data is synthesized from cylindrical wave scattering data in the first step and the object profile is reconstructed in the second step using the parallel beam (plane wave) filtered backpropagation algorithm on the synthesized plane wave data. The second algorithm combines these two steps into a single "fan beam filtered backpropagation algorithm." In this method the reconstruction of the object profile is obtained by summing reconstructions corresponding to a single fixed location of the source, over the source point locations.

The results presented in the paper apply only to two-dimensional objects; i.e., objects whose properties are constant in one direction. They are readily extended, however, to the three-dimensional case. This extension can be performed in two ways. The first of these simply requires that the measurement boundary  $\Sigma$  be replaced by a surface  $\hat{\Sigma}$  formed by sweeping the  $\Sigma$  boundary along the perpendicular to the plane in which  $\Sigma$  lies. Thus, for example, for the case of a circular boundary  $\hat{\Sigma}$  is a circular cylinder while for a line boundary  $\hat{\Sigma}$  becomes a plane surface. The treatment presented in the paper then applies for three-dimensional objects enclosed by  $\hat{\Sigma}$  if the two-dimensional scattered field measurements performed over  $\hat{\Sigma}$  are **projected** onto the boundary  $\Sigma$ . The resulting reconstruction will be of a projection of the three-dimensional object profile onto the plane formed by  $\Sigma$  so that a full three-dimensional reconstruction will require a sequence of experiments employing measurement surfaces having different orientations relative to the object. In the case of fan beam insonification, the source boundary  $\Sigma_0$  must always remain in the same plane as the boundary  $\Sigma$ . This first method is the generalization, to the case of arbitrary measurement boundaries, of the three-dimensional reconstruction method presented in Section 4 of [4].

The theory and algorithms presented here can also be generalized to the three-dimensional case directly. By this we mean that all the fundamental equations can be replaced by their three-dimensional equivalents. For example, in three-dimensions the plane wave scattering amplitude is defined by

$$f(\underline{s}, \underline{s}_0) = k^2 \int d^3r O(\underline{r}) \psi(\underline{r}; \underline{s}_0) e^{-ik \hat{s} \cdot \underline{r}}, \quad (25)$$

where now  $\underline{r} = (x, y, z)$  and  $\underline{s} = (s_x, s_y, s_z)$ . Eqs. (4)-(8) are similarly generalized to the three-

dimensional case. The three-dimensional form of the inversion formula (9) is given by [14,18].

$$O_{LP}(\underline{r}) = -\frac{k}{(2\pi)^4} \int d\Omega_{s_0} \int d\Omega_s |s - s_0| f(s, s_0) e^{ik(s - s_0) \cdot \underline{r}}, \quad (26)$$

where  $d\Omega_{s_0}$  and  $d\Omega_s$  are differential solid angles and the integrals are over  $4\pi$  steradians. By employing Eq. (26) together with the appropriate three-dimensional generalization of the expressions for the scattering amplitude given in table I, three-dimensional reconstruction algorithms analogous to those given in Table II can be readily obtained.

#### APPENDIX A - DERIVATION OF EQ. (12)

We begin by setting  $\psi(\underline{r})$  in Eq. (1) equal to the sum of an insonifying wave  $\psi^{(i)}(\underline{r})$  and a scattered wave  $\psi^{(s)}(\underline{r})$ . Since the insonifying wave satisfies the homogeneous Helmholtz equation; i.e., Eq. (1) with  $O(\underline{r}) = 0$ , we find that

$$(\nabla^2 + k^2)\psi^{(s)}(\underline{r}) = k^2 O(\underline{r})\psi(\underline{r}). \quad (A.1)$$

We can obtain a relationship between the scattered field  $\psi^{(s)}$  and its normal derivative  $\frac{\partial}{\partial n}\psi^{(s)}$  evaluated on the boundary  $\Sigma$  by making use of Eq. (A.1) and the fact that  $\exp(-ik\underline{s} \cdot \underline{r})$  satisfies the homogeneous Helmholtz equation, i.e.,

$$(\nabla^2 + k^2)e^{-ik\underline{s} \cdot \underline{r}} = 0. \quad (A.2)$$

Multiplying Eq.(A.1) by  $\exp(-ik\underline{s} \cdot \underline{r})$  and (A.2) by  $\psi^{(s)}(\underline{r})$  and subtracting the resulting equations yields

$$\begin{aligned} e^{-ik\underline{s} \cdot \underline{r}} \nabla^2 \psi^{(s)}(\underline{r}) - \psi^{(s)}(\underline{r}) \nabla^2 e^{-ik\underline{s} \cdot \underline{r}} \\ = k^2 O(\underline{r})\psi(\underline{r})e^{-ik\underline{s} \cdot \underline{r}}. \end{aligned} \quad (A.3)$$

Integrating with respect to  $\underline{r}$  throughout the volume of space bounded by  $\Sigma$  and applying Green's theorem then yields

$$k^2 \int d^2r O(\underline{r})\psi(\underline{r})e^{-ik\underline{s} \cdot \underline{r}} = \int_{\Sigma} dl \left\{ e^{-ik\underline{s} \cdot \underline{r}} \frac{\partial}{\partial n} \psi^{(s)}(\underline{r}) - \psi^{(s)}(\underline{r}) \frac{\partial}{\partial n} e^{-ik\underline{s} \cdot \underline{r}} \right\}. \quad (A.4)$$

In this equation  $\frac{\partial}{\partial n}$  denotes differentiation along the outward normal to the boundary  $\Sigma$  and  $dl$  is the differential element of length on this boundary. Putting

$$\frac{\partial}{\partial n} e^{-ik\underline{s} \cdot \underline{r}} = -ik \hat{n} \cdot \underline{s} e^{-ik\underline{s} \cdot \underline{r}}, \quad (A.5)$$

we finally obtain

$$\begin{aligned} k^2 \int d^2r O(\underline{r})\psi(\underline{r})e^{-ik\underline{s} \cdot \underline{r}} \\ = \int_{\Sigma} dl \left[ \frac{\partial}{\partial n} \psi^{(s)}(\underline{r}) + ik \hat{n} \cdot \underline{s} \psi^{(s)}(\underline{r}) \right] e^{-ik\underline{s} \cdot \underline{r}} \end{aligned} \quad (A.6)$$

which is the desired result.

#### APPENDIX B - DERIVATION OF EQ. (21)

The wavefield  $\psi(\underline{r}'; \underline{r})$  generated by a line source centered at  $\underline{r}'$  satisfies the equation

$$\left[ \nabla_{\underline{r}}^2 + k^2 - k^2 O(\underline{r}') \right] \psi(\underline{r}; \underline{r}') = \delta(\underline{r} - \underline{r}'), \quad (B.1)$$

where  $\nabla_{\underline{r}'}^2$  denotes the Laplacian operator in the  $\underline{r}'$  coordinates. The field  $\psi(\underline{r}'; \underline{s}_0)$  generated by the insonifying plane wave  $\exp(ik\underline{s}_0 \cdot \underline{r}')$  satisfies

$$\left[ \nabla_{\underline{r}'}^2 + k^2 - k^2 O(\underline{r}') \right] \psi(\underline{r}'; \underline{s}_0) = 0. \quad (\text{B.2})$$

Upon multiplying Eq.(B.1) by  $\psi(\underline{r}'; \underline{s}_0)$  and Eq. (B.2) by  $\psi(\underline{r}; \underline{r}')$  and subtracting the two resulting equations yields

$$\begin{aligned} \psi(\underline{r}'; \underline{s}_0) \nabla_{\underline{r}'}^2 \psi(\underline{r}; \underline{r}') - \psi(\underline{r}; \underline{r}') \nabla_{\underline{r}'}^2 \psi(\underline{r}'; \underline{s}_0) \\ = \psi(\underline{r}'; \underline{s}_0) \delta(\underline{r} - \underline{r}'). \end{aligned} \quad (\text{B.3})$$

Integrating (B.3) over the region of space bounded by  $\Sigma_0$  and applying Green's theorem then yields

$$\psi(\underline{r}; \underline{s}_0) = \int_{\Sigma_0} dl_0 \left\{ \psi(\underline{R}_0; \underline{s}_0) \frac{\partial}{\partial n_0} \psi(\underline{r}; \underline{R}_0) - \psi(\underline{r}; \underline{R}_0) \frac{\partial}{\partial n_0} \psi(\underline{R}_0; \underline{s}_0) \right\}, \quad (\text{B.4})$$

where  $\underline{R}_0$  denotes a point on  $\Sigma_0$ ,  $dl_0$  is the differential element of length on  $\Sigma_0$  and  $\frac{\partial}{\partial n_0}$  the derivative along the outward normal to the boundary.

If in the integrand of (B.4) we decompose  $\psi(\underline{R}_0; \underline{s}_0)$  into the sum of the insonifying field  $\exp(ik\underline{s}_0 \cdot \underline{r})$  plus the scattered field  $\psi^{(s)}(\underline{R}_0; \underline{s}_0)$  we obtain

$$\psi(\underline{r}; \underline{s}_0) = I + \int_{\Sigma_0} dl_0 \left\{ \frac{\partial}{\partial n_0} \psi(\underline{r}; \underline{R}_0) - ik \hat{n}_0 \cdot \underline{s}_0 \psi(\underline{r}; \underline{R}_0) \right\} e^{ik\underline{s}_0 \cdot \underline{R}_0} \quad (\text{B.5})$$

where

$$I = \int_{\Sigma_0} dl_0 \left\{ \psi^{(s)}(\underline{R}_0; \underline{s}_0) \frac{\partial}{\partial n_0} \psi(\underline{r}; \underline{R}_0) - \psi(\underline{r}; \underline{R}_0) \frac{\partial}{\partial n_0} \psi^{(s)}(\underline{R}_0; \underline{s}_0) \right\}. \quad (\text{B.6})$$

The integral in Eq. (B.6) can be shown to be independent of the exact boundary  $\Sigma_0$ . Moreover, if we take  $\Sigma_0$  to infinity it must vanish since both  $\psi^{(s)}(\underline{R}_0; \underline{s}_0)$  and  $\psi(\underline{r}; \underline{r}_0)$  satisfy the Sommerfeld radiation condition. It follows that

$$\psi(\underline{r}; \underline{s}_0) = \int_{\Sigma_0} dl_0 \left\{ \frac{\partial}{\partial n_0} \psi(\underline{r}; \underline{R}_0) - ik \hat{n}_0 \cdot \underline{s}_0 \psi(\underline{r}; \underline{R}_0) \right\} e^{ik\underline{s}_0 \cdot \underline{R}_0}. \quad (\text{B.7})$$

If we substitute Eq. (B.7) into the definition of the plane wave scattering amplitude (3) we obtain

$$f(\underline{s}, \underline{s}_0) = k^2 \int d^2\tau O(\underline{r}) e^{-ik\underline{s} \cdot \underline{r}} \int_{\Sigma_0} dl_0 \left\{ \frac{\partial}{\partial n_0} \psi(\underline{r}; \underline{R}_0) - ik \hat{n}_0 \cdot \underline{s}_0 \psi(\underline{r}; \underline{R}_0) \right\} e^{ik\underline{s}_0 \cdot \underline{R}_0}. \quad (\text{B.8})$$

Interchanging orders of integration and making use of the definition (8) of the cylindrical wave scattering amplitude then leads finally to the desired result; viz.,

$$f(\underline{s}, \underline{s}_0) = \int dI_0 \left\{ \frac{\partial}{\partial n_0} \gamma(\underline{s}; \underline{R}_0) - ik \hat{n}_0 \cdot \underline{s}_0 \gamma(\underline{s}; \underline{R}_0) \right\} e^{ik\underline{s}_0 \cdot \underline{R}_0}. \quad (\text{B.9})$$

## REFERENCES

- [1] Mueller, R. K., Kaveh, M., and Wade, G., Reconstructive tomography and applications to ultrasonics, *Proc. IEEE* 67, 567-587 (1979).
- [2] Greenleaf, J. F. and Bahn, R. C., Clinical imaging with transmissive ultrasonic computerized tomography, *IEEE Trans. Biomed. Eng. BME-28*, 177-185 (1981).
- [3] Greenleaf, J. F., Computerized tomography with ultrasound, *Proc. IEEE* 71, 330-337 (1983).
- [4] Devaney, A. J., A filtered backpropagation algorithm for diffraction tomography, *Ultrasonic Imaging* 4, 336-350 (1982).
- [5] Devaney, A. J., A computer simulation study of diffraction tomography, *IEEE Trans. Biomed. Eng. BME-30*, 377-386 (1983).

- [6] Lipson, H. and Cochran, W., *The Determination of Crystal Structures* (Cornell University Press, Ithaca, NY, 1966).
- [7] Vainshtein, B. K., *Diffraction of X-rays by Chain Molecules* (John Wiley, NY, 1974).
- [8] Devaney, A. J., Inverse source and scattering problems in ultrasonics, *IEEE Trans. Sonics Ultrasonics*, SU-30, 355-364 (1983).
- [9] Wolf, E., Three-dimensional structure determination of semi-transparent objects from holographic data, *Opt. Commun.* 1, 153-156 (1969).
- [10] Porter, R., Determination of structure of weak scatterers from holographic images, *Opt. Commun.* 39, 362-364 (1981).
- [11] Mueller, R. K., Kaveh, M., and Inversion, R. D., A New Approach to Acoustic Tomography Using Diffraction Techniques, in *Acoustical Imaging Vol. 8*, A. F. Metherell, ed., pp. 615-628 (Plenum Press, New York, 1980).
- [12] Pan, S. X. and Kak, A. C., A computational study of reconstruction algorithms for diffraction tomography, *IEEE Trans. Acoustics, Speech and Signal Processing* (to appear).
- [13] Slaney, Malcolm and Kak, A. C., Diffraction tomography, in *Inverse Optics*, A. J. Devaney, ed., *Proc. SPIE Vol. 413*, pp. 2-19 (1983).
- [14] Beylkin, G., The fundamental identity for iterated spherical means and the inversion formula for diffraction tomography and inverse scattering, *J. Math. Phys.* 24, 1399-1400 (1983).
- [15] Morse, P. M. and Feshbach, H., *Methods of Theoretical Physics, Vol. I* (McGraw-Hill, New York, 1953).
- [16] Beylkin, G. and Devaney, A. J., Theory of diffraction tomography within the Born and Rytov approximations, submitted to *J. Math. Phys.*
- [17] Kak, A. C., Computerized tomography with x-ray emission and ultrasound sources, *Proc. IEEE* 67, 1245-1272 (1979).
- [18] Devaney, A. J., Inversion formula for inverse scattering within the Born approximation, *Opt. Lett.* 7, 111-112 (1982).